

Using a Virtual Reality Environment to Simulate the Pushing of Cylindrical Nanoparticles

A. H. Korayem¹, A. K. Hoshiar², N. N. Ashtiani¹, and M. H. Korayem¹

1- School of Mechanical Engineering, Iran University of Science & Technology, Tehran, I. R. Iran

2- Faculty of Industrial and Mechanical Engineering, Islamic Azad University, Qazvin Branch, Qazvin, I. R. Iran

(*) Corresponding author: hkorayem@iust.ac.ir

(Received: 05 Dec. 2013 and accepted: 12 Aug. 2014)

Abstract:

With the rise in the use of AFM (Atomic Force Microscope), we have witnessed a growing use of atomic microscope based nanorobots in the precise displacement of various particles. There are certain limitations to the application of nanorobots in the moving of nanoparticles. One of the most important of these limitations is the lack of an appropriate image feedback concurrent with the displacing process; thus, the design of a graphical interface is essential in this regard. In this paper, the displacement of a cylindrical nanoparticle in a straight path, and in the air medium, has been simulated by means of a virtual reality graphical interface. This simulation is actually aimed at eliminating the previously stated limitation through the use of a graphical interface. The procedure has been presented in seven stages and the relevant diagrams of each stage have been extracted. Then, the obtained diagrams have been interpreted and discussed. In the end, by using the experimental results and the existing simulations for spherical particles, the presented results have been validated.

Keywords: Nanoparticles displacement process, Cylindrical nanoparticles, AFM nanorobot, Virtual reality.

1. INTRODUCTION

In this paper nanomanipulation refers to pushing cylindrical nano particle, with a higher-than-nanometer accuracy, by the actuator (cantilever) of an AFM nanorobot (Figure 1) [1]. Since it is impossible to observe and touch nano-scale objects, the virtual reality graphical interfaces will enable the users of these interfaces to acquire a correct knowledge and understanding of nano environments.

The moving and displacing of nanoparticles is aimed at producing materials, tools and systems with new functions and characteristics required

by the existing necessities. To achieve the above goals, we need to establish a proper relationship between the macro domain and the molecular and atomic domains, and this necessitates the existence of graphical interfaces through which the scientists and researchers can gain a deeper understanding of the displacement process.

The moving and displacing of cylindrical nanoparticles in a laboratory setting is performed by pushing them with the help of an AFM nano robot's actuator tip. The displacement operation can be performed in different mediums such as vacuum, air and liquid. In the present paper, a virtual reality environment has been developed for

the displacement of cylindrical particles in the air medium. With the lack of simultaneous observation of the manipulation process, the virtual reality environment makes it possible to explore the conditions of motion of cylindrical nanoparticles before performing the experimental procedure.

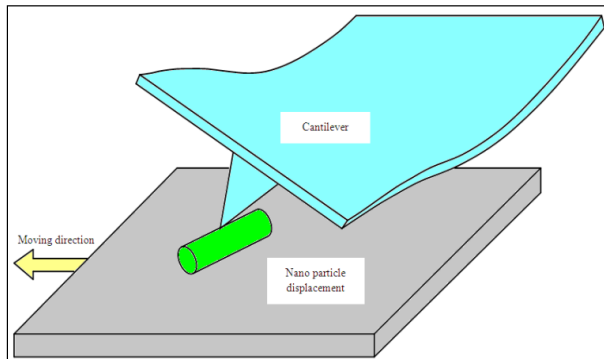


Figure 1: Schematic view of manipulation process of cylindrical nano particle

The early works on the displacement of nanoparticles were conducted on spherical particles. These activities then provided the groundwork for the investigation of cylindrical nanoparticles. Schaefer performed the displacement of spherical particles for the first time by using AFM [2]. Then, Falvo presented a report on the displacement of carbon nanotubes by means of AFM.

In addition to reviewing the mechanical properties of carbon nanotubes, he observed that when these particles make proper contact with the actuator, their motion modes change from rotating and sliding to other motion modes such as the rolling mode [3]. In the described research works, the displacement operations have been performed manually and without the use of modeling and simulation.

Sitti conducted the first research work on the dynamic modeling of spherical nanoparticles displacement. In his model, he presented the pushing of nanoparticles [4]. Subsequently, Korayem investigated the mechanical characteristics of AFM actuator for a more effective and secure displacement of nanoparticles [5]. As the displacement of cylindrical nanoparticles became widespread, Xi *et al.* presented a model for the displacement of nanotubes on electrode by means

of an AFM nanorobot [6].

Following that, the prediction of the motion modes of cylindrical particles and their displacement was studied [7, 8]. Moradi investigated the manner of movement of cylindrical nanoparticles while considering the size effect in the 2D case [9]. Korayem and Hoshair introduced a 3D model for manipulation of cylindrical nano particle. In the recent works, dynamic and motion modes were widely investigated [10, 11]. In all the mentioned researches, in spite of presenting various motion models for the displacement of spherical and cylindrical nanoparticles, the virtual reality medium which establishes an appropriate connection between the macro and nano worlds, has not been used.

By introducing a model and assuming a spherical probe tip, Sitti was able to simulate the forces and deformations three-dimensionally and to produce the image of the substrate at the same time [12]. Then, since it was impossible to observe the process of nanoparticles displacement, Korayem did some research to predict the sizes of particles that could be transferred by this method [13]. In fact, the main reason for the creation of a virtual reality environment is that a probe is not able to move the particles and perform imaging at the same time. A virtual reality environment was designed for spherical particles in which the nanoparticles could be moved and the displacement process can be observed simultaneously [14].

This virtual reality environment was later expanded to include the use of actuators with different geometries (rectangular, dagger-shaped, triangular and V-shaped) in the displacement operation [15, 16]. Subsequently, a graphical interface was presented which produces 3D images of the nano-world.

In this technique, a tactile tool with one degree of freedom and a common 2D mouse were used in the main manipulator. By utilizing this graphical interface, the feedback of forces could be obtained as well [17]. In the most recent work, the possibility of drift problem was investigated [18]. To reduce uncertainty during the pushing process, a stochastic predictive model was applied [19]. Moreover, a sequential parallel pushing method

was used for more effective pushing strategy and new toll was used to overcome sliding problems of tip [20, 21]. The simulations presented in the introduced works were for the spherical particles. In this paper, the virtual reality environment and the motion simulations associated with that have been adapted to the process of cylindrical nanoparticles displacement.

2- KINEMATIC AND DYNAMIC MODELING

Since the elastic deformations are negligible, they can be disregarded, and the kinematic free-body diagram of the actuator can be sketched according to Figure 2. To better display the deformations, they have been enlarged in the drawings. It should be mentioned that the figures and relations presented in this section have been obtained by expanding the existing relations for the displacement of spherical particles [5, 10, 11, 13, and 14].

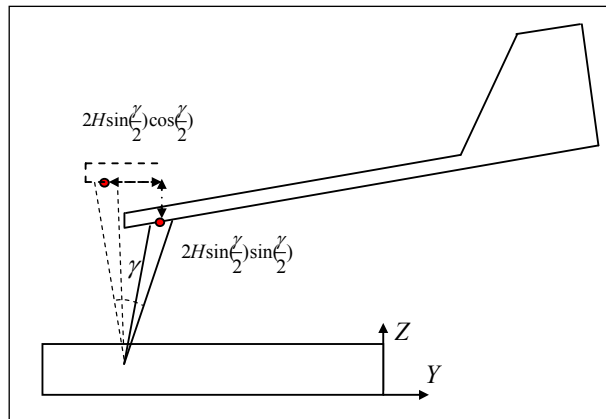


Figure 2: Investigating the kinematics of motion in the 3D state

$$\ddot{Y}_p = H\ddot{\gamma} \cos\left(\frac{\gamma}{2}\right) - H\ddot{\gamma} \sin^2\left(\frac{\gamma}{2}\right) - 2H\dot{\gamma} \sin\left(\frac{\gamma}{2}\right) \cos\left(\frac{\gamma}{2}\right) \quad (1)$$

$$\ddot{Z}_p = -H\ddot{\theta} \sin\theta + H\dot{\theta}^2 \cos\theta - 2H\dot{\gamma} \cos\left(\frac{\gamma}{2}\right) \sin\left(\frac{\gamma}{2}\right) - H\dot{\gamma}^2 \cos^2\left(\frac{\gamma}{2}\right) + H\dot{\gamma}^2 \sin^2\left(\frac{\gamma}{2}\right) \quad (2)$$

$$\ddot{X}_p = -H\ddot{\theta} \cos\theta + H\dot{\theta}^2 \sin\theta \quad (3)$$

To present the dynamic model governing the displacement of these particles, the free-body diagram of the actuator should be sketched. The external forces applied on the probe tip are F_x , F_y and F_z , which produce the internal forces and moments of V , W , M_{θ_x} , M_{θ_y} , F_x , F_y and F_z . The required accelerations have been determined with regard to the dynamic model [11].

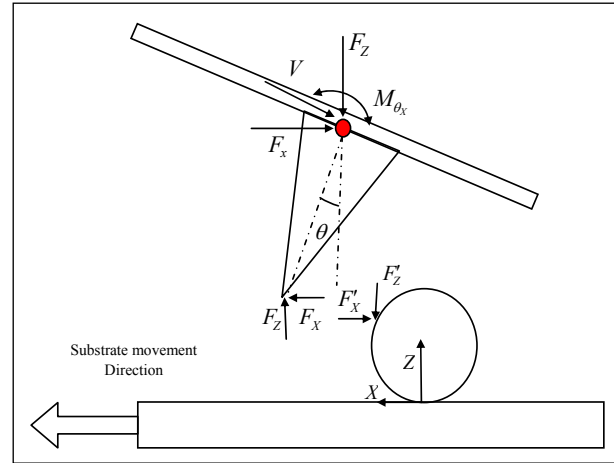


Figure 3: Forces applied on the actuator (front view)

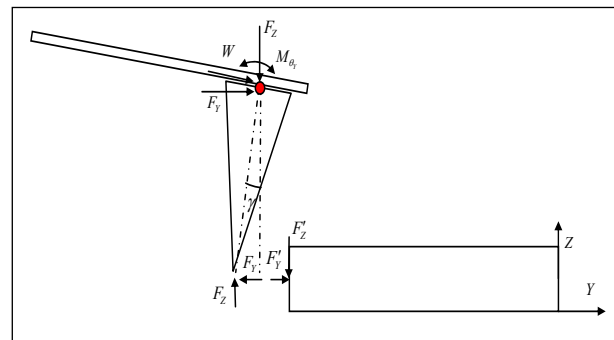


Figure 4: Forces applied on the actuator (side view)

$$F_x = ma_x + F_x + V \cos \theta \quad (4)$$

$$F_y = \left(\frac{I\ddot{\gamma} + M_{\theta_y}}{H} \right) \cos \gamma - F_z \sin \gamma \cos \gamma - V \sin \theta \sin \gamma \cos \gamma - ma_z \sin \gamma \cos \gamma - ma_y \sin^2 \gamma + F_y \sin^2 \gamma \quad (5)$$

$$F_z = \left(\frac{I\ddot{\theta} + M_{\theta_x}}{H} \right) \sin \theta - ma_x \sin \theta \cos \theta - F_x \sin \theta \cos \theta + F_z \cos^2 \theta + ma_z \cos^2 \theta + W \sin \gamma \cos^2 \theta \quad (6)$$

Two different regions have been considered for modeling the probe tip-particle contact (δ_t) and also the particle-substrate contact (δ_s).

The contact between probe tip and particle, because of the size of the contact area and the no-effect of the nano particle length, is very similar to the contact between two spheres, which has been investigated in previous works. Therefore, the spherical mode of the JKR model has been used to simulate the probe tip-particle contact [9, 10]. The contact between cylinder and flat surface is modeled by means of the JKR relations presented for cylindrical contact; and the contact radius, a_s is obtained from the following equations [9, 10, 22]:

$$a_t^3 = \frac{3R}{4K} \left[P + 3w\pi R + \sqrt{6w\pi R P + (3w\pi R)^2} \right] \quad (7)$$

$$w = \left[\frac{3\pi k a_s^2 l}{8R} - P \right] \quad (8)$$

$$6\pi k a_s l^2$$

In the presented relations, K is the equivalent modulus of elasticity, R is the equivalent radius, L is the length of contact surface, W is the surface energy and P is the force normal to the surface. Force is the only variable parameter, and the changes of contact radius for a specific surface are obtained in proportion to it. It should be noted that it is not possible to solve relation (8) analytically. Hence, by arrangement based on a_s , for different forces (P), a numerical solution is presented by using MATLAB software, and the a_s values are determined accordingly. Also, by knowing the contact radiuses (a_t) and a_s , the indentation values, δ_t and δ_s are determined with using the following relations:

$$\delta_t = \frac{a_t^2}{R} - \frac{2}{3} \sqrt{\frac{6\pi w a_t}{K}} \quad (9)$$

$$\delta_s = \frac{a_s^2}{R} - \frac{2}{3} \sqrt{\frac{6\pi w a_s}{K}} \quad (10)$$

3- SIMULATING THE DISPLACEMENT PROCESS OF CYLINDRICAL NANOPARTICLES

First, the physical parameters and the characteristics of materials, probe and substrate are specified and input into the simulation process as constants. In the presented simulations, the contact angle between probe tip and particle has been considered as 60°.

Table 1: Surface features in the displacement of nanoparticles

Surface energy (ω)	Surface adhesion (τ)	Surface friction (μ)
$.2 \frac{J}{m^2}$	28M.pa	.8

Table 2: Specifications of the AFM actuator

Module of elasticity (E)	Radius of probe's tip (ν)	probe's density (ρ)
169(Gpa)	20 n.m	2330 ($\frac{kg}{m^3}$)

Nanotube radius: In order to obtain clearer images during the displacement of nanoparticles, radius of 50 nm has been considered for the nanotubes. However, for the validation and comparison of data, radius of 30 nm has been used in all the relations and diagrams. Nanotube length: In order to obtain clearer images during the displacement of nanoparticles, length of 200 nm has been considered for the nanotubes. However, for the validation and comparison of data, length of 1.8 μ m has been used

in all the relations and diagrams.

The designed virtual reality environment is introduced step by step. The steps for the transfer of nanoparticles have been presented in 7 phases. The most important step in the moving operation of nanoparticles is the step of establishing contact between probe tip and particle until reaching the threshold of movement, which is covered in phase 5. It should be noted that the time duration shown for each phase is exclusively allocated to that phase; and to get the total time for the nanoparticles displacement operation, these separate times should be summed up.

Phase 1- In the first phase of the program, the user is asked to choose the number of particles between 1 and 15. Then using the facilities provided, the user himself enters these particles into the program's environment.

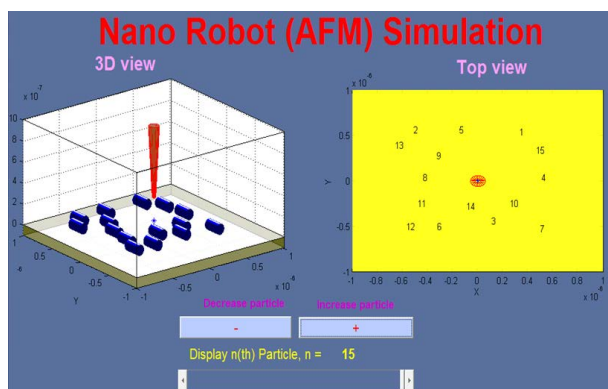


Figure 5: The first phase of the program and introducing the particles into the environment

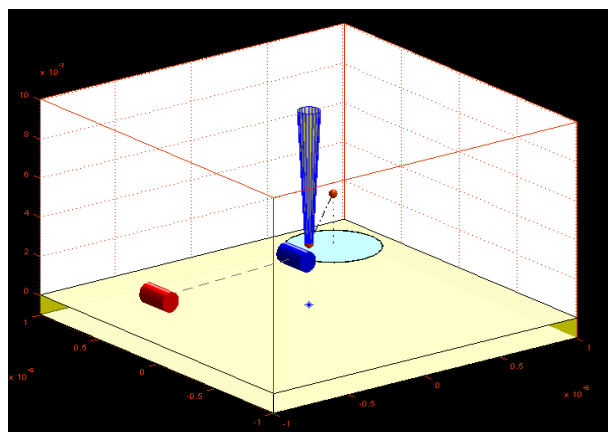


Figure 6: Implementing the second phase of the program and determining the desired coordinates

Phase 2- In this phase, first, the user selects the target particle. Then, he can determine the particle's secondary location by using the provided facilities.

Phase 3- After determining these coordinates, it is time to move the probe. It should be pointed out that the probe is situated in the middle of the substrate, and at a safe height (h_{safe}), in order to prevent it from hitting the nanotubes. In this phase, the probe starts to move and comes to rest at a location close to the nanotube. This distance has been chosen so that the probe can make contact with the nanotube from every direction.

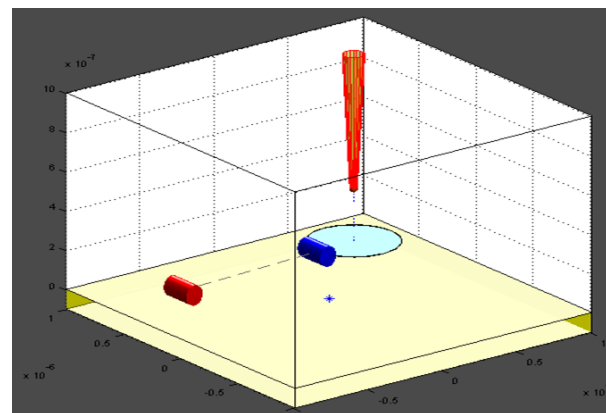


Figure 7: Implementing the third phase of the program and moving the probe tip

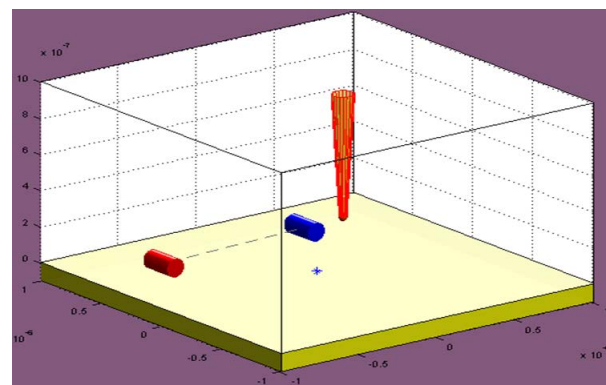


Figure 8: Implementing the fourth phase of the program and adjusting the probe height

Phase 4- In this phase, the height of the probe tip is adjusted for establishing the contact. To have a defined height, it is necessary to determine a reference; so, the substrate is considered as the reference. Now, the probe is moved downward until

its tip contacts the substrate. This point indicates the zero location. Following the contact, the probe moves up to a specific height.

Phase 5- After determining an appropriate height for the probe, it is time to make the contact, which is the most important and sensitive stage of the operation. Since it is possible for the probe tip and also the nanotube to get damaged when contact is made, the speed of probe movement is reduced to 10 nm/s. Therefore in this phase of the program, first, the probe moves to make contact with the particle. Then, this contact continues until the nanotube is on the verge of movement, but the particle doesn't yet move.

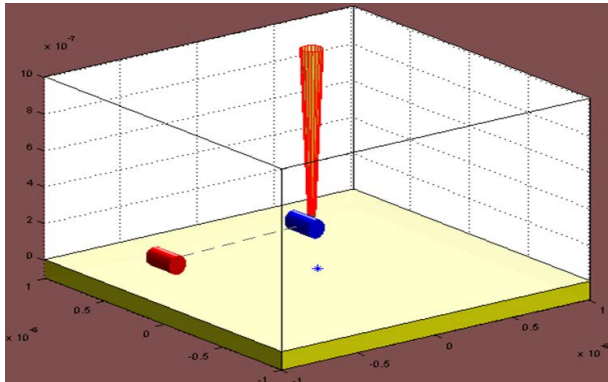


Figure 9: Implementing the fifth phase of the program, establishing contact, and reaching the movement threshold

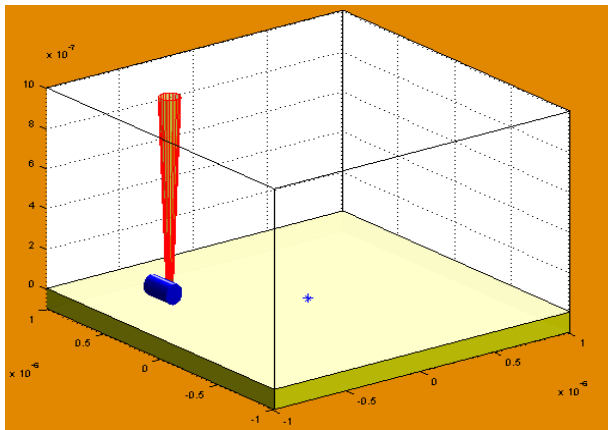


Figure 10: Implementing the sixth phase of the program and transferring the nanoparticle to the desired coordinates

Phase 6- All the events in this phase of nanoparticles displacement occur after reaching the movement

threshold. The particle on the verge of movement starts to move with the slightest application of force. Thus, the probe begins to move with a constant velocity and transfers the particle to the considered location.

Phase 7: The last stage of nanoparticle displacement is the return of the probe to its initial location, i.e., the center of substrate.

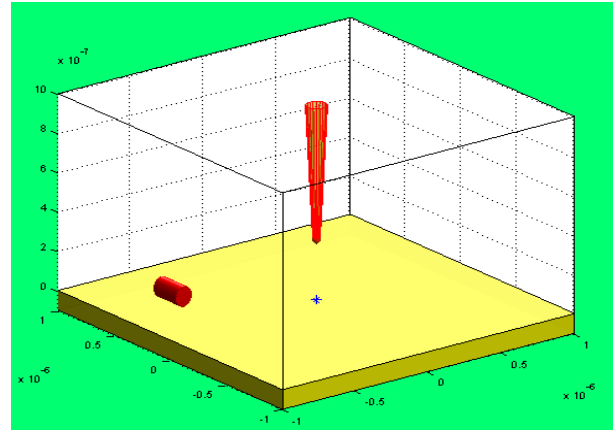


Figure 11: Implementing the seventh phase of the program and returning the probe to its initial location

4- ANALYZING THE RESULTS AND DIAGRAMS

In this section, the presented diagrams are analyzed. It should be mentioned that in the first and second phases, only the virtual reality environment is created, and there are no diagrams to be analyzed. In phases 3 through 6, the changes of force and the location of probe tip can be observed and investigated by the operator. In the third phase, the probe is moved to a position suitable for pushing the nanotube. In the fourth phase, the height of the probe is adjusted for making the contact and in the fifth phase, the probe contacts the particle and proceeds to the threshold of movement. Then, in the sixth phase, the particle is moved to the considered location. No diagram has been presented for the final phase in which the probe returns to its initial location.

Plotting and analyzing the diagrams of the third phase: As we previously mentioned, in this phase,

only the probe is displaced from the center of substrate to a suitable location for the moving of particle. So it is obvious that the force diagrams should have values of zero.

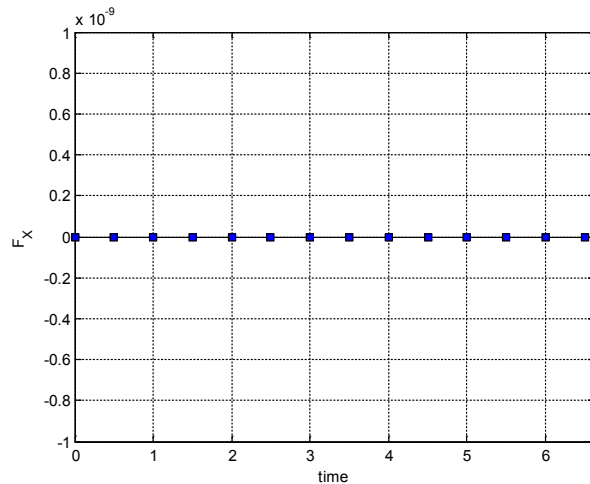


Figure 12: Changes of forces with time in the third phase of nanoparticles displacement

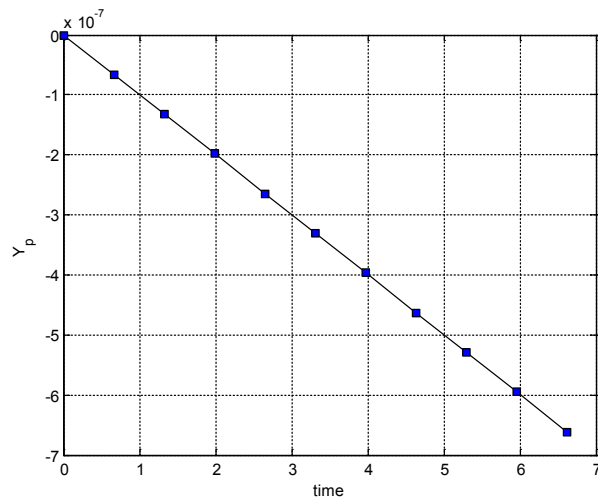


Figure 13: Change in X direction (to transfer the nanoparticle to the target point)

From Figure 15, it is observed that the height of probe from the substrate doesn't change, and the probe remains at the same initial height (h_{safe}). Since, at this stage, the probe doesn't contact the particle or the substrate, all the forces and the indentation depth in the contact of probe tip and particle are zero, and the indentation depth and the contact radius in the contact between particle and substrate remain at their initial values.

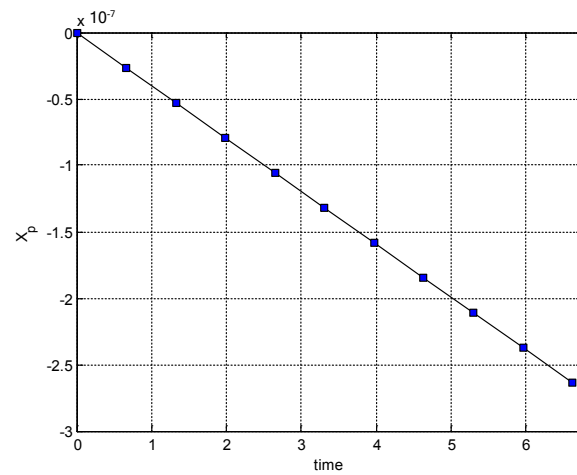


Figure 14: Change in Y direction (to transfer the nanoparticle to the target point)

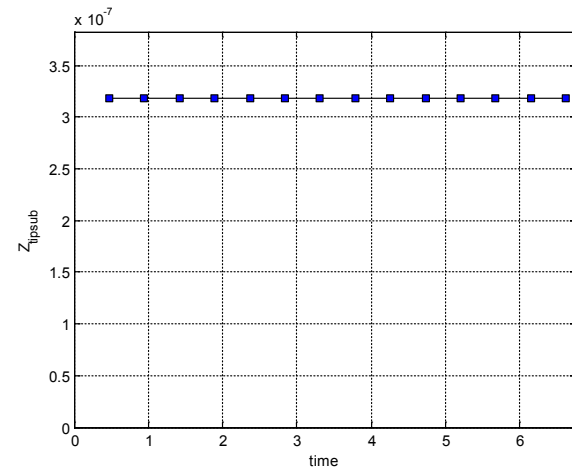


Figure 15: Displacement along the 'z' in the third phase of the movement at height 'h'

Plotting and analyzing the diagrams of the fourth phase: This phase shows the steps to determine the h_{set} . In this phase, as in the preceding phase, the probe and nanotube have no contact with each other; therefore, the diagrams of forces along the 'x' and 'y' directions are like Figure 12, with values of zero. The only difference between the diagrams in this phase and the previous phase is the time duration of the process.

A sudden jump is observed in the F_z diagram (Figure 16), which can be explained as follows: as long as the probe tip does not contact the substrate, no force exists along this direction. At the moment of contact between probe tip and substrate, force F_{z0} is created,

and when the probe moves upward and separates from the surface, this force becomes zero again. The magnitude of force F_{z0} depends on the shape of the actuator [15, 16].

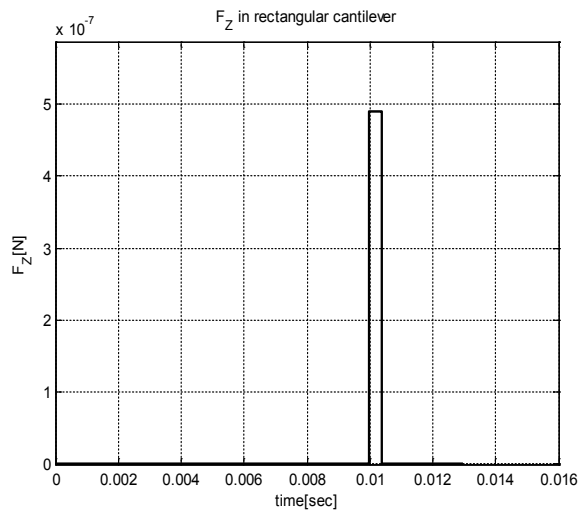


Figure 16: Changes of F_z during the implementation of the fourth phase of the program

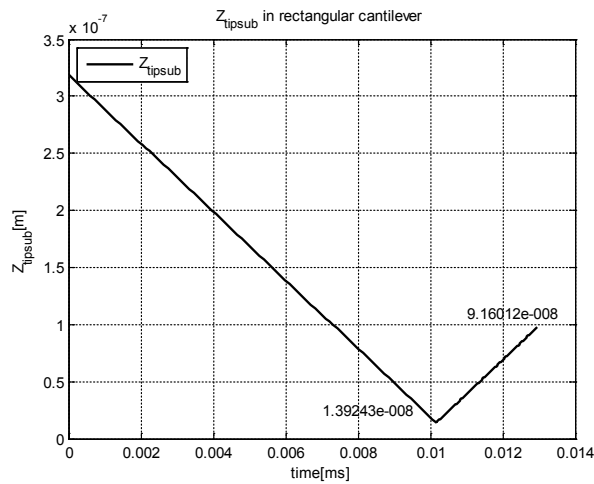


Figure 17: Changes of the probe tip coordinates along the z direction

At this stage, in a fixed location, we can witness changes along the 'z' to reach the height desired for the operation. The displacement along the 'z' is in a back and forth manner. According to Figure 17, first, the probe impacts the substrate and then it rises. Due to this impact with the substrate, δ_{tip} is created which typically indicates the deformation

between the probe tip and substrate (Figure 18).

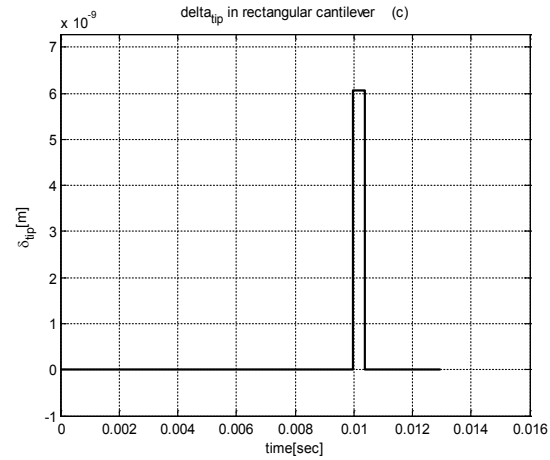


Figure 18: Changes of δ_{tip} with time in the fourth phase of nanoparticles displacement

Plotting and analyzing the diagrams of the fifth phase: In this phase, since the probe moves along the 'x' and 'y' to establish contact with the probe, no displacement occurs along the 'z'. When contact is made, all the forces change along all three 'x', 'y' and 'z' directions. These forces increase until the nanotube reaches the movement threshold. The changes of F_z from the moment of contact to the movement threshold are so negligible that it can be disregarded.

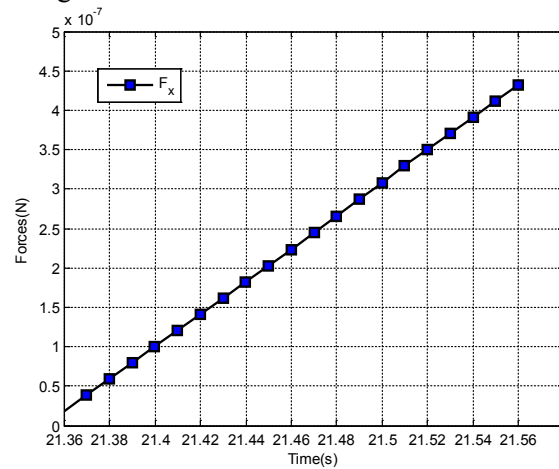


Figure 19: Changes of F_x with time in the fifth phase of nanoparticles displacement

Due to the contact between particle and probe tip and the emergence of forces, some indentation is

created between probe tip and particle, which is designated by δ_{tip} . The amount of this indentation increases with the increase of forces. Also, due to the existence of a force along the 'z', the indentation between particle and substrate, which is shown by δ_{sub} , changes as well. However, since the changes of F_z are negligible, the changes of δ_{sub} from the moment of contact until the movement threshold can be overlooked. The diagrams plotted in Figures 25 and 26 illustrate the radius of contact between particle and substrate and between particle and probe tip, respectively.

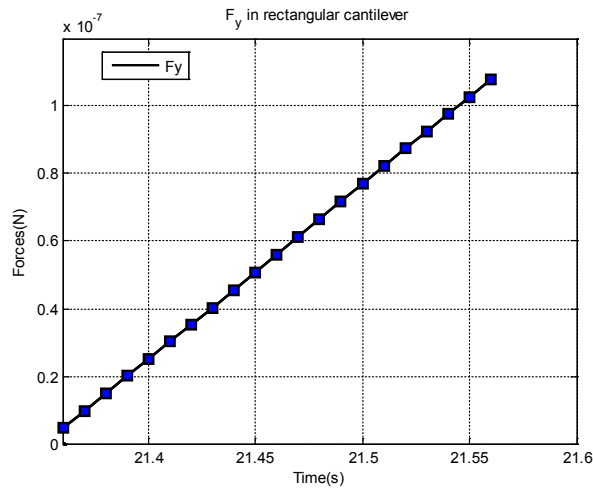


Figure 20: Changes of F_y with time in the fifth phase of nanoparticles displacement

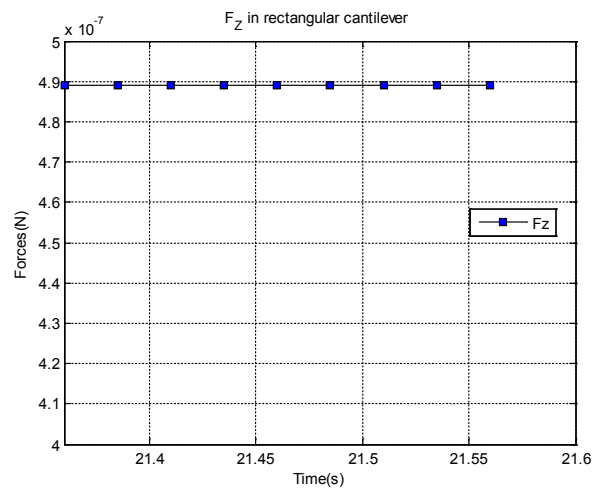


Figure 21: Changes of F_z with time in the fifth phase of nanoparticles displacement

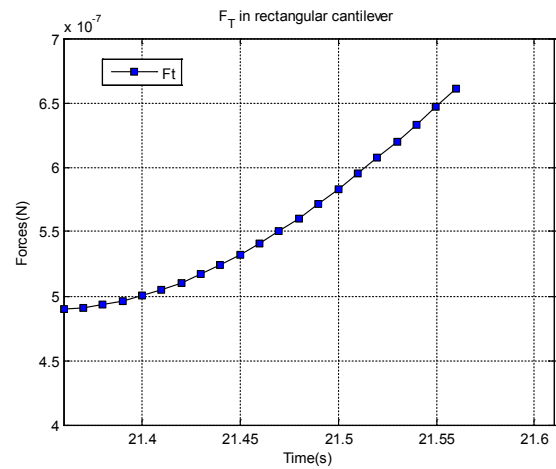


Figure 22: Changes of F_T with time in the fifth phase of nanoparticles displacement

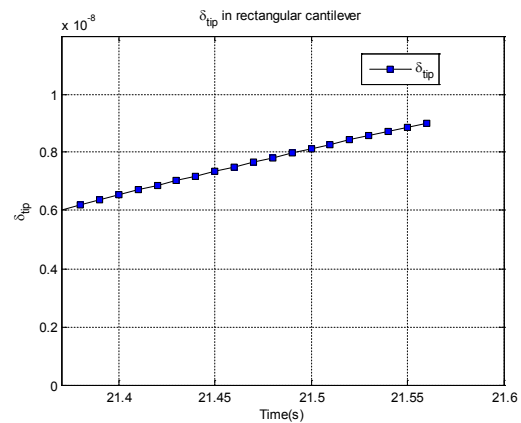


Figure 23: Changes of δ_{tip} with time in the fifth phase of nanoparticles displacement

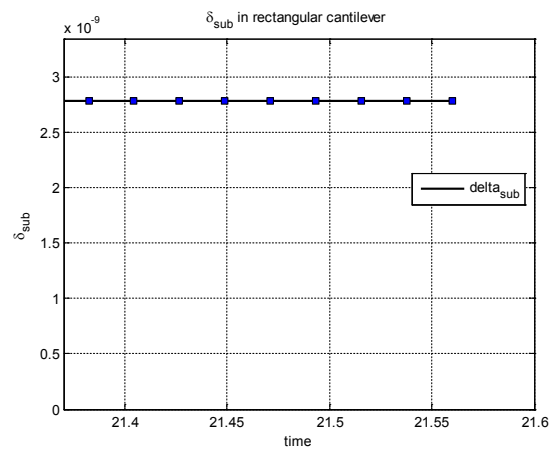


Figure 24: Changes of δ_{sub} with time in the fifth phase of nanoparticles displacement

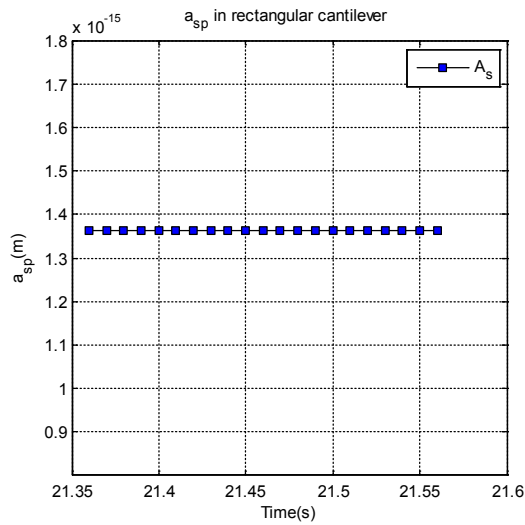


Figure 25: Changes of the particle-substrate contact radius

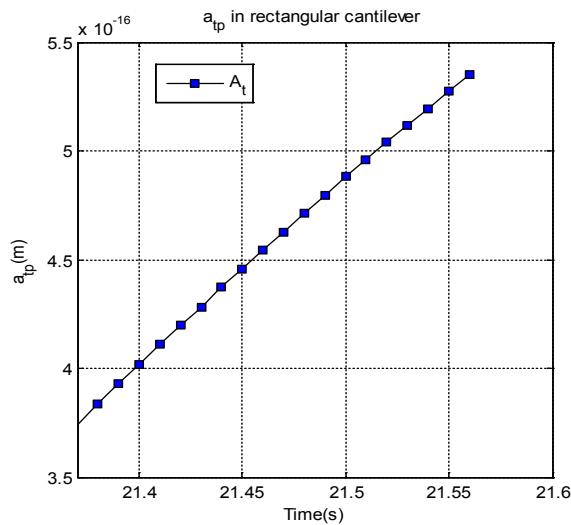


Figure 26: Changes of the probe-particle contact radius

Plotting and analyzing the diagrams of the sixth phase: Since the particle is displaced with a constant velocity, no acceleration is created and in this phase, all the forces have constant values. Also, assuming that the nanotube moves in a straight path, only coordinate 'x' of the particle changes in this phase. The presented results were compared with the results obtained experimentally for the displacement of cylindrical particles, and for particles with a length of 1.8 μm and a diameter of 100 nm. These results show an adequate agreement. In these experiments,

the cylindrical particles were pushed by the tip of the AFM actuator and the obtained results match the dynamic diagrams presented in this article for similar particles shown in figure [23].

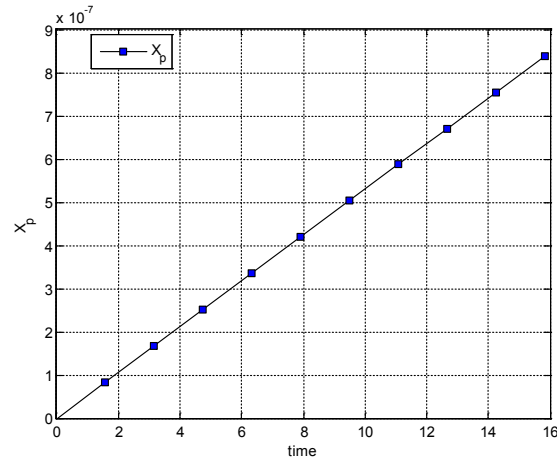


Figure 27: Changes of the particle 'x' coordinate with time in the sixth phase of the program

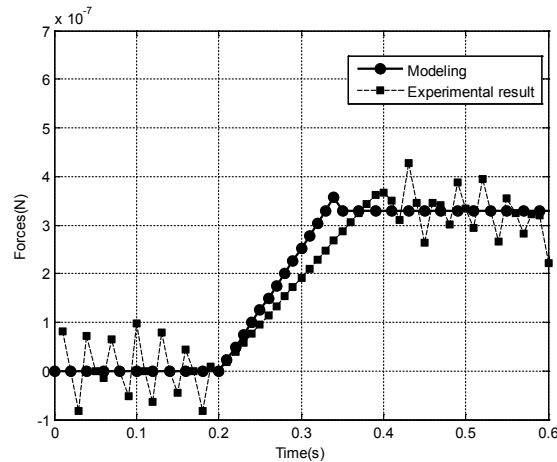


Figure 28: Comparing the experimental [23] and simulation results of critical force and time for the manipulation of cylindrical particles

5- CONCLUSION

To remove the distance between the real macro-world and the nano-world environment, it is important to create a virtual reality environment that can convey a real sense to the one who uses the medium. In this paper a new 3D simulation of cylindrical nano particle manipulation in virtual

reality environment has been introduced. The use of a virtual reality environment is a practical way of overcoming human limitations.

As stated earlier, by means of the presented environment all the forces and displacements can be observed during the manipulation operation and a correct knowledge of what goes on in the process is achievable. The simulation demonstrate that for a particle with radius of 50 nm and length of 10 nm the dynamic mode is slides; however, for particles with longer length (a particle with radius of 50 nm and length of 1.0 μm length) the spinning mode is the dominant mode with a critical force of 1.8 μN . The most effective parameter in manipulation process is the nanoparticle radius; in case of increasing it from 20 to 100 nm, a large increases in critical motion force can be observed (2×10^{-9} to 1×10^{-8} N) which indicates the impact of geometrical parameters on motion modes. In this way, by knowing the duration of operation and the forces created during the displacement of nanoparticles, a highly precise manipulation can be implemented.

REFERENCES

1. T. J. Lopenen, Introduction to Microsystems: Nano-manipulation, proceedings of the seminar held in the course Introduction to Microsystems, (2007), pp. 1-10.
2. D. M. Schaefer, R. Reifenberger, A. Patil, R. P. Andres, Fabrication of Two-Dimensional Arrays of Nanometer-Size Clusters with the Atomic Force Microscope, Applied Physic Letters, Vol. 66, (1995), pp.1012-1014.
3. M. R. Falvo, J. Steele, R. M. Taylor, R. Superfine, Gear like Rolling Motion Mediated by Commensurate Contact: Carbon Nanotubes on HOPG, Physical Review B, Vol. 62, (2000), pp.10665-10667.
4. M. Sitti, H. Hashimoto, Controlled Pushing of Nanoparticles: Modeling and Experiments, IEEE/ASME Transactions on Mechatronics, Vol. 5, (2000), pp.199-211.
5. K. Daeinabi, M. H. Korayem, Nano-Manipulator Force Transducer Modeling Based on Atomic Force Microscopy, 9th IEEE Conference on Nanotechnology, (2000), pp.896 - 899.
6. L. Lianqing, Y. Peng, T. Xiaojun, W. Yuechao, D. Zaili, N. Xi, Force Analysis of Top down Forming CNT Electrical Connection Using Nano-manipulation Robotics, IEEE International Conference on Mechatronics and Automation, (2006), pp.113-117.
7. J. Hsu, S. Chang, Surface Adhesion between Hexagonal Boron Nitride Nanotubes and Silicon Based on Lateral Force Microscopy, Applied Surface Science, Vol. 256, (2010), pp.1769-1773.
8. Z. Deng, E. Yenilmez, Nanotube Manipulation with Focused Ion Beam, Applied Physics Letters, Vol. 88, (2006), pp.023119-023121.
9. M. Moradi, A. H. Fereidon, S. Sadeghzadeh, Aspect ratio and dimension effects on nanorod manipulation by atomic force microscope, Micro & Nano Letters, Vol. 5, (2010), pp. 324 – 327.
10. M. H. Korayem, A. K. Hoshidar, Modeling and simulation of dynamic modes in the manipulation of nanorods, Micro & Nano letters, Vol. 8, No. 6, (2013), pp. 284-287.
11. M. H. Korayem, A. K. Hoshidar, Dynamic 3D modeling and simulation of nanoparticles manipulation using an AFM nanorobot, Robotica, Vol. 32, (2014), pp. 625-641.
12. M. Sitti, Teleoperated and Automatic Nano-manipulation Systems Using Atomic Force Microscope Probes, IEEE Conference on Decision and Control, Vol. 3, (2003), pp. 2118-2123.
13. M. H. Korayem, A. K. Hoshidar, N. Ebrahimi, Maximum Allowable Load of Atomic Force Microscope (AFM) Nano-robot, The International Journal of Advanced Manufacturing Technology, Vol. 43, (2009), pp.690-700.
14. M. H. Korayem, S. Esmailzadehha, Virtual reality interface for nano-manipulation based on enhanced images, The International Journal of Advanced Manufacturing Technology, Vol. 63, No. 9-12, (2012), pp. 1153-1166.
15. M. H. Korayem, S. Esmailzadehha, N. Rahmani, M. Shahkarami, Nano Manipulation with rectangular Cantilever of atomic force microscope (AFM) in a virtual reality environment, Digest journal of nanomaterials and biostructures, Vol. 43, (2012), pp. 435-445.
16. N. Rahmani, Virtual reality environment for AFM based nano manipulation with different cantilever

- geometry, M.Sc Thesis, Islamic Azad University of Qazvin, (2010).
17. A. Ferreira, C. Mavroidis, Virtual Reality and Haptics for Nano-Robotics, IEEE Robotics & Automation Magazine, Vol. 13, No. 3, pp.78-92.
 18. G. Li, Y. Wang, L. Liu, Drift compensation in AFM-Based nanomanipulation by strategic local scan, Transaction on automation science and engineering, Vol. 9, (2012), pp. 755-762.
 19. Z. Wang, L. Liu, Z. Wang, Z. Dong, S. Yuan, J. Hou, A stochastic state prediction in AFM based nanomanipulation, International Conference on Mechatronics and Automation, (2012), pp. 1335-1340.
 20. K. Xu, A. Kalantari, X. Qian, Efficient AFM-Based nanoparticle manipulation via sequential parallel pushing, Transaction on nanotechnology, Vol. 11, (2012), pp. 666-675.
 21. J. Hou, L. Liu, Z. Wang, Z. Wang, N. Xi, Y. Wang, C. Wu, Z. Dong, S. Yuan, AFM-Based robotic nano-hand for stable manipulation at nanoscale, Transaction on automation science and engineering, Vol. 10, (2013), pp. 285-295.
 22. D. A. Dillard, A.V. Pocius, The mechanics of adhesion, Elsevier science, (2002). pp. 1-44.
 23. J. H. Hsu, S. H. Chang, Tribological interaction between multi-walled carbon nanotubes and silica surface using lateral force microscopy, Wear, Vol. 266, (2009), pp. 952-959.